






Article

# Creating Landscape-Scale Site Index Maps for the Southeastern US Is Possible with Airborne LiDAR and Landsat Imagery

Ranjith Gopalakrishnan <sup>1,\*</sup>, Jobriath S. Kauffman <sup>2</sup>, Matthew E. Fagan <sup>3</sup>, John W. Coulston <sup>4</sup>, Valerie A. Thomas <sup>5</sup>, Randolph H. Wynne <sup>5</sup>, Thomas R. Fox <sup>6</sup> and Valquiria F. Quirino <sup>5</sup>

<sup>1</sup> Department of Forest Sciences, University of Eastern Finland, 80101 Joensuu, Finland

<sup>2</sup> Conservation Management Institute, Virginia Tech, Blacksburg, VA 24061, USA; jkauffma@vt.edu

<sup>3</sup> Department of Geography and Environmental Systems, University of Maryland, Baltimore County 1000 Hilltop Circle, Baltimore, MD 21250, USA; mfagan@umbc.edu

<sup>4</sup> USDA Forest Service (Southern Research Station), Blacksburg, VA 24061, USA; jcoulston@fs.fed.us

<sup>5</sup> Department of Forest Resources and Environment Conservation, Virginia Tech, Blacksburg, VA 24061, USA; thomasv@vt.edu (V.A.T.); wynne@vt.edu (R.H.W.); valquiria.quirino@mnstate.edu (V.F.Q.)

<sup>6</sup> Rayonier Inc., Forest Research Center, P.O. Box 819, Yulee, FL 32041, USA; tom.fox@rayonier.com

\* Correspondence: ranjith.gopalakrishnan@uef.fi

Received: 8 January 2019; Accepted: 26 February 2019; Published: 6 March 2019



**Abstract:** Sustainable forest management is hugely dependent on high-quality estimates of forest site productivity, but it is challenging to generate productivity maps over large areas. We present a method for generating site index (a measure of such forest productivity) maps for plantation loblolly pine (*Pinus taeda* L.) forests over large areas in the southeastern United States by combining airborne laser scanning (ALS) data from disparate acquisitions and Landsat-based estimates of forest age. For predicting canopy heights, a linear regression model was developed using ALS data and field measurements from the Forest Inventory and Analysis (FIA) program of the US Forest Service ( $n = 211$  plots). The model was strong ( $R^2 = 0.84$ , RMSE = 1.85 m), and applicable over a large area (~208,000 sq. km). To estimate the site index, we combined the ALS estimated heights with Landsat-derived maps of stand age and planted pine area. The estimated bias was low (−0.28 m) and the RMSE (3.8 m, relative RMSE: 19.7%, base age 25 years) was consistent with other similar approaches. Due to Landsat-related constraints, our methodology is valid only for relatively young pine plantations established after 1984. We generated 30 m resolution site index maps over a large area (~832 sq. km). The site index distribution had a median value of 19.4 m, the 5th percentile value of 13.0 m and the 95th percentile value of 23.3 m. Further, using a watershed level analysis, we ranked these regions by their estimated productivity. These results demonstrate the potential and value of remote sensing based large-area site index maps.

**Keywords:** forestry; forest site productivity; site index; Landsat; airborne laser scanning; forest productivity mapping; FIA

## 1. Introduction

Spatially explicit maps of forest productivity are compelling to forest stakeholders for several reasons. First, sustainable forest management is generally highly dependent on site productivity measures as they significantly influence silviculture-related decisions such as treatment and harvesting schedules [1,2]. In particular, accurate forest productivity maps, especially those delineating poor productivity areas, can provide salient inputs for *precision forestry*, such as spatially specific management interventions (such as fertilization, herbaceous weed control and density management)

on forest stands [3]. Second, forests in the southeastern part of the United States constitute large carbon stocks (estimated at around 36% of conterminous U.S. forest carbon [4]) and they absorb a sizable amount (around 13%) of regional greenhouse gas emissions [5]. However, some model-based estimates under climate change scenarios suggest that the magnitude of these carbon sinks could be significantly diminished in the future in the face of climate change [6]. Hence, there is a need to better understand current forest productivity levels at local and regional scales. To monitor forest site productivity (the potential of a site to produce biomass; see [7]) accurately, spatially extensive maps are needed that can be updated over time. Finally, spatially extensive site productivity maps are also useful for calibrating models related to land-use and land surface processes [8,9].

Site index (SI) is defined as the average total height that dominant and co-dominant trees are projected to reach in well-stocked, even aged stands at a given base age (usually 25 or 50 years) [10]. Site classification by such stand height (i.e., site index curves) has become a universal practice in forestry and is recognized as one of the most suitable indicators of site productivity in even-aged forest stands [7]. A sizable proportion (around 30%) of southeastern US forests are dominated by the genus *Pinus* ("pine"), with around 10 million hectares in naturally regenerated stands and another 14 million hectares in plantations [11,12].

The spatial distribution of forest productivity or site index in this region has been studied over the past three decades using two distinct approaches: the theoretical model approach and sampling based approach. The theoretical model approach consists of developing spatially explicit models for pine forests in this region. Parametric and non-parametric empirical models that relate measured site index to biophysical variables (climate, edaphic, and physiographic factors) on a large scale have been developed [13]. A version of the dynamic, process-based 3PG model customized for loblolly pine has been developed and validated over a range of sites in Georgia, USA [14]. However, in these efforts, the prediction estimates are *potential productivity* or the productivity under the assumed plantation coverage area and management regimes. A different value of productivity might actually manifest on the landscape, known as *expressed site productivity*. This is the productivity which results after silvicultural treatments [15]. A promising method to make potential productivity estimates more realistic is to constrain model parameters using observational data via data assimilation techniques [16]. Of course, the quality of such an exercise depends on the amount, quality and sample representation of available observations.

In the sampling plot based approach, the variation of expressed pine productivity over a wide area in the Southeast is analyzed using plot-level field-measured data. For example, Jokela et al. [17] analyzed seven studies across the natural range of loblolly pine to examine factors that control and limit the productivity of managed stands. Another similar region-wide study of thirteen loblolly pine plantations spanning seven southern states and four physiographic provinces primarily looked at the effects of controlling competing vegetation [18]. Changes in expressed site productivity over the geographic range of loblolly pine were reported by Zhao et al. [11], detailing an extensive analysis that involved six long-term studies and over 250 plots.

However, while there have been quite a few sampling plot based studies, the potential of remote sensing techniques for site index prediction for this region has not been studied. The generation of a site index map for a relatively large area by such techniques would identify regional spatial trends in productivity and help to target management interventions in low-productivity forest stands. There has been prior work regarding prediction and verification of site index from ALS data in other regions. One of the first articles that describes explicit ALS-based site index mapping was by Gatzliolis (2007) for a temperate rainforest site [19]. Wulder et al. [20] combined ALS-measured tree heights with inventory age information to predict site index for a 2500-ha forested area in British Columbia, Canada. Tompalski et al. [21] detailed a more involved study in the same region, where both ALS and Landsat time-series data were used together to predict site index over 100 square km of western hemlock dominated forests (RMSE = 5.55 m). In a recent study, Kandare et al. [22] outlined a method by which both age and dominant height were predicted using ALS and hyperspectral data, which was then used

for site index estimation. Stand register-based age data has been combined with single-date [23,24] and multitemporal [25] ALS data to generate spatial maps of site index. As part of a study conducted at the Clemson experimental forest in USA, Lidar-derived site index estimates were compared to those from field soil-survey data [26] (41 forest stands involved). The authors reported significant differences between these two estimates for loblolly pine, but less so for some other species.

However, none of these ALS-based studies address the unique challenges of the southeastern USA, namely: (1) The lack of a homogeneous, large-area ALS acquisition effort, thus necessitating the need to combine disparate ALS projects (acquired mostly for non-forestry purposes with diverse sensors and acquisition parameters); (2) The lack of standardized planting records for deriving stand age (as those used in [19,20,23–25]); and (3) A heterogeneous management landscape. In other words, the area involved in our study is much larger than the previous ones (hundreds to thousands of square kilometers, in our case), with accompanying issues and challenges.

In this study, we focus on even-aged, planted pine forests managed at varying levels of intensity. Recent work relevant to the unique challenges of the Southeast was described by Gopalakrishnan et al. [27], where it was shown that accurate models of dominant canopy height could be formulated over as much as 76 disparate ALS projects. Further, they also showed that canopy heights are better predicted for softwoods and over more homogeneous forested areas, as has been done by others [28,29]. We leverage on these two key insights in the design of this present study. Moreover, forest ages can be predicted with reasonable accuracy for a large area in the southeastern USA using Landsat time series data [30]. Furthermore, such time series data can be combined with other spectral data to identify planted pines [31]. Repeated ALS data collection is planned for this area in the future; the United States Geological Survey (USGS) is coordinating an inter-agency effort aiming to periodically collect ALS data for the conterminous United States [32], thus adding to the relevance of our work.

The objective of the present study is to determine whether site index for loblolly pine could be accurately estimated and mapped using disparate discrete return ALS datasets combined with Landsat-derived estimates of forest stand age. We try to answer the following specific research questions:

1. How effective is ALS data collected via disparate projects coupled with Landsat-based forest age products in predicting site index for pine plantations?
2. What is the distribution and regional spatial pattern of site productivity?

Hence, by asking these questions, we aim to evaluate ALS data collected over large areas (mainly for topographical mapping) as another tool that can be used to understand and analyze local and regional trends in southeastern USA forest productivity.

## 2. Methods

### 2.1. Study Area

Our study area focused on all even-aged pine plantation forests in the area of ALS coverage (see Figure 1). The selection criteria for the ALS projects used are explained below.

### 2.2. Remote Sensing Datasets

The following three datasets were used in our study:

1. ALS data: We considered many ALS data acquisition projects that: (1) were available in the public domain as of 2011; (2) were from the southeastern states of the USA; (3) had recorded multiple returns (i.e., two or more) for each pulse; and (4) contained at least one FIA plot with pine plantation, in their area of coverage (see below). This resulted in 38 projects being finally selected, spread across eight southeastern states (Virginia, North Carolina, South Carolina, Georgia, Florida, Alabama, Mississippi and Texas), as shown in Figure 1. We used georeferenced point-cloud data

from these projects. Their acquisition dates ranged from 2005 to 2012, and 31 of these projects used instruments capable of recording up to four returns.

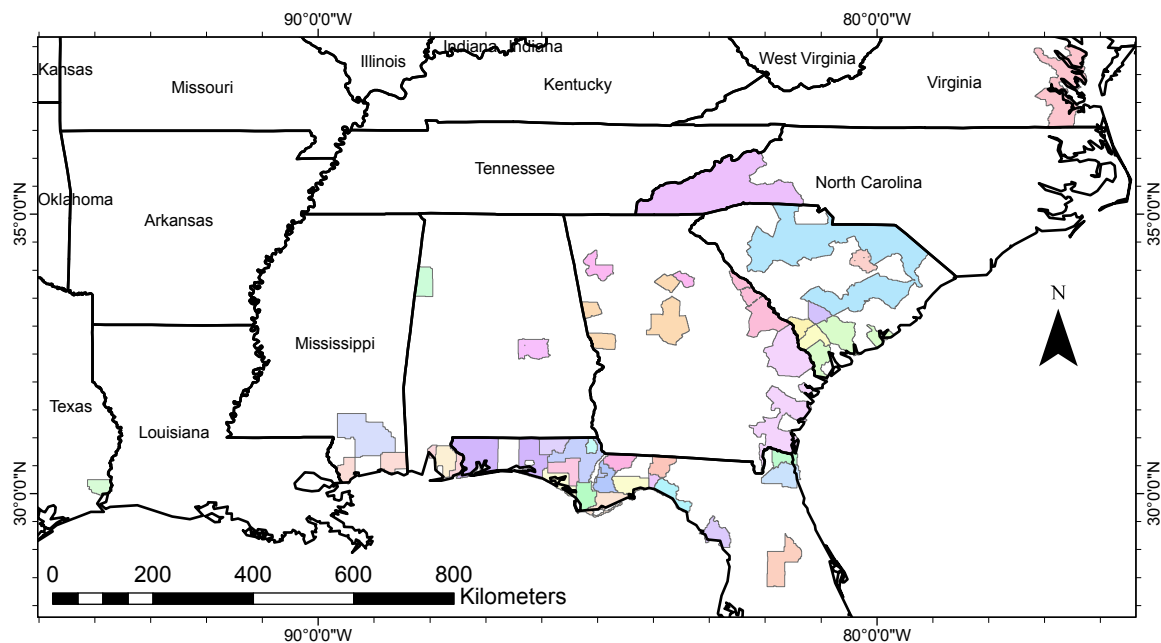


**Figure 1.** ALS data from 38 projects spread across eight states of USA were used in this study. Each project is shown in a different color. The total land area covered by these projects is approximately 208,000 sq. km. This region is dominated by loblolly pine, with some slash pine (*Pinus elliottii* Engelm.) in the extreme south.

2. Landsat-based prediction of plantation age: The vegetation change tracker (VCT) algorithm is a fairly well-established and extensively tested technique that effectively leverages multitemporal Landsat data (both Landsat 5 TM and Landsat 7 ETM+; 1984–2011) to detect disturbances to forest stands (such as clearcutting) [33]. Recently, additional steps that partitioned such disturbances into stand-clearing ones (i.e., clearcuts) and non-stand-clearing ones (such as thinning, insect damage and ice damage) were proposed as part of an enhanced vegetation change tracker algorithm (henceforth, eVCT) [30]. Identifying and demarcating the stand-clearing disturbance helps delineate the stand, and the number of years since disturbance is a good proxy for stand age. All pixels in a particular delineated stand are given a single value of year of disturbance (and hence, age).
3. Landsat-based identification of planted pine stands: We used a map of planted pine forest stands in the southeastern USA generated by a combination of spectral and multitemporal Landsat data [31]. The following were the prominent datasets used in this classification: (1) National Land Cover Database 2011, a Landsat-based land cover map; (2) summer and winter Normalized Difference Vegetation Index (NDVI) (and their difference) from Landsat; (3) the 30 m resolution global forest change dataset by Hansen et al. [34] (2000–2013); and (4) the Vegetation Change Tracker dataset (VCT; 1985–2011 [33]). A decision tree model was developed using these datasets as well as a combination of plot-level forest type data and Google Earth imagery for training and verification. From the generated map, it was estimated that about 28% of the total forest area of southeastern USA is covered by pine plantations.

### 2.3. Canopy Height Model

We first developed an ALS-based dominant canopy height model for pine plantations that was applicable over the ALS coverage area shown in Figure 1. The field data for this effort came from the

Forest Inventory and Analysis (FIA) of the United States Forest Service [35]. We used FIA's *phase 2* (P2) plots. Figure 2 shows the nationally standardized layout for these plots. As part of the inventory, all standing trees of diameter at breast height greater than or equal to 12.7 cm (5.0 inches) are measured or estimated for tree height. The stated accuracy of such field height measurements is  $\pm 10\%$ . This is expected, as field height was measured using clinometers and there are limitations to these instruments in closed-canopy forest conditions. We also had access to the field-recorded GPS co-ordinates of the plot centers (i.e., unaffected by "fuzzing and swapping"), thus co-registration of these plots with ALS data was good.

We used a square plot size 30 m to cut out the ALS point cloud; this size was chosen as the other two Landsat-based data sources had map resolutions of 30 m. This plot was oriented such that two edges were along the north–south direction, and two along the east–west direction. The position of this square ALS plot with respect to the FIA plot elements is shown in Figure 2. The corresponding field plot for this effort is *subplot 1* from the FIA, a circular plot of 7.32 m (24.0 feet) radius, centered at the center of the FIA plot.

We applied the following criteria to select FIA plots in the Southeast region, as per our domain of interest (planted pine forests):

1. The plots had to be *single-condition*. "Condition" is a term used by the FIA to refer to major land-use types on the plots [35]. A consequence of FIA's plot center randomizing strategy is that some plots can straddle multiple land-use types (e.g., a plot may be 70% pine stand, 20% hardwoods stand, and 10% water). Hence, we filtered out such non-homogeneous plots.
2. The plot was marked to have clear evidence of artificial regeneration (i.e., it is a plantation).
3. The pine species basal area of the plot (percent) was  $\geq 95\%$  of total basal area on the plot.
4. ALS data within two years from the year of visit and measurement of the FIA plots are available. That is, there is a maximum of  $\pm 2$  years difference between the years of ALS acquisition and of FIA field measurement.

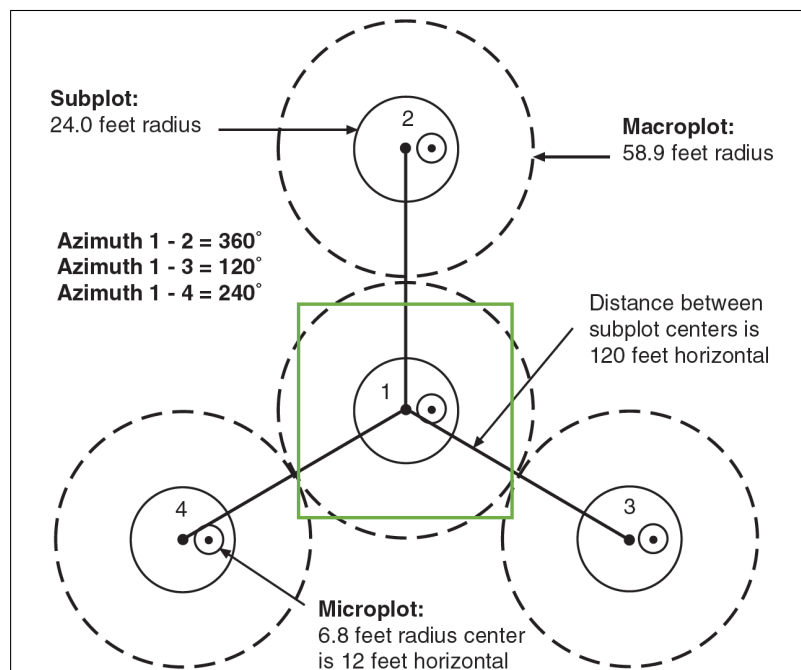


**Figure 2.** The ALS plot (green outline) in reference to the FIA plot (black markings). Figure adapted from [35].

After applying these conditions and after screening out plots that were either clear-cut between field measurements and ALS acquisition and plots with few uneven-aged trees, we had 211 FIA

plots left, spanning 38 different ALS projects. We extracted ALS plot point clouds for each of these 211 FIA plots from our ALS data using lastools (<http://rapidlasso.com/lastools/>). At this point, one should note that co-registration errors are an issue given that GPS instruments used by FIA are not survey-grade. However, McRoberts et al. [36] reported that most positional errors are within 15.0 m, and later estimated that most are within 7.0 m (M. Russell, personal communication, October 2015). Hence, the relatively large size of the ALS plot (compared to the FIA center subplot) and the homogeneous nature of the forest stands selected (i.e., were single-condition) addresses the co-registration issue adequately (to a large extent). Some of the salient ALS acquisition related statistics are given in Figure 3 for a better understanding of the quality of lidar data available over these plots.

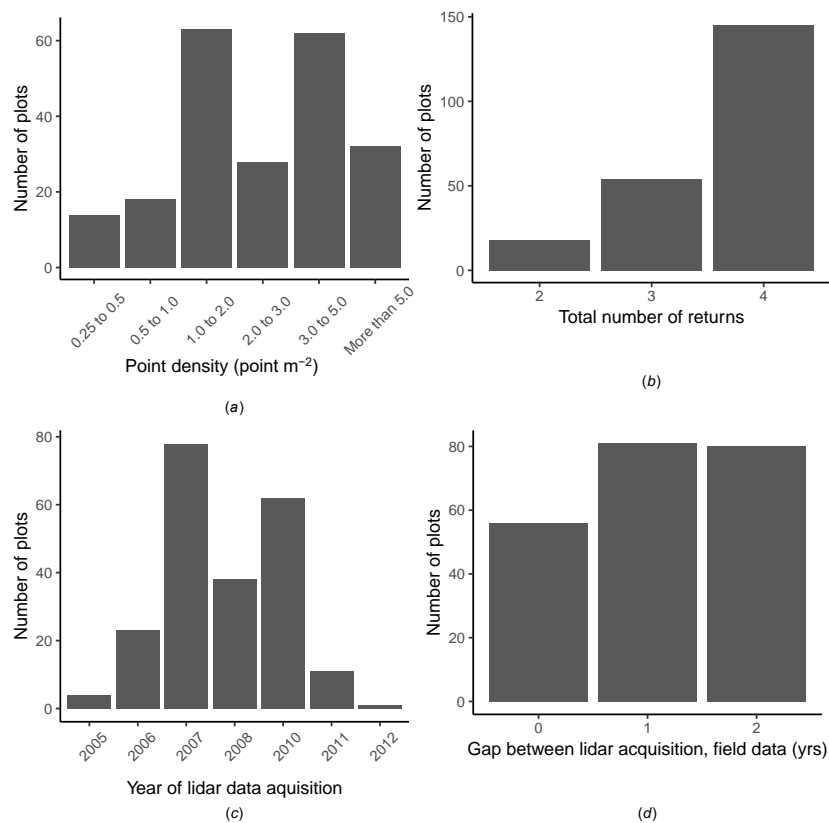


**Figure 3.** The distribution of some notable ALS acquisition parameters over the selected FIA plots. (a) Point density. The actual value calculated on the plot is shown here, which may be significantly different from the ALS project’s documented nominal point spacing based value. The median point density is 2.6 pts m<sup>-2</sup>. (b) Total number of returns labeled. For example, “1” means that the acquisition was based on a single-return system. (c) Year of ALS data acquisition. (d) Gap (in years) between the ALS data acquisition and FIA field measurement (absolute value). Around 37% of plots had a measurement lag within  $\pm 1$  year.

For each ALS point cloud (corresponding to the ALS plots), we derived the canopy height using the following processing steps:

1. Ground classification, using the lasground tool of lastools (<http://rapidlasso.com/lastools/>).
2. The understory points were identified, using a threshold of 3.0 m. This threshold was determined after inspecting 12 FIA plots (of the 211) for which understory height information was available from the FIA.
3. ALS distributional metrics: The standard percentiles of height above ground ( $h_5, h_{10}, h_{20}$ , etc.) were extracted from the point cloud (using MATLAB v7.14, 2012), after excluding understory points.

- The dominant height of all trees on our field plot (*subplot 1* of the FIA) was calculated as the average height of the five tallest trees on that subplot. We used the FIA's *HT* variable, in the *TREE* table.

At this point, we had a set of square ALS plots of 30 m size with associated field-measured dominant heights. First, pairwise correlations between the percentiles of height ( $h_5, h_{10}, h_{20}$ , etc.) and the plot level dominant height were examined to select the most correlated percentile metric. Then, an OLS (ordinary least squares) based bivariate linear regression model was developed between this metric and the field-measured dominant height. We avoided a direct estimation of dominant height from ALS height percentiles (e.g., see [20]) to avoid systematic, project-dependent bias in height estimation. This was also motivated by considering the differences in acquisition types and prevalence of low point density (see Figure 3). We instead depended on field plot data and regression models to generate dominant heights from ALS data, thus closely following the methodology outlined by White et al. [37].

#### 2.4. Generation of a Sample Site Index Map from ALS and Landsat Data

The generation of canopy height maps for the entire ALS coverage area shown in Figure 1 was beyond the scope of this initial study, especially as it would involve processing a relatively large amount of data (a few terabytes). Hence, we decided to concentrate on the smaller region shown in blue in Figure 4. These two regions had large, contiguous LiDAR coverage, were geographically well-separated and represented a wide range of site conditions. We generated site index maps for all pixels labeled as planted pine by Fagan et al. [31] in this region. Here, plantations are almost always of the loblolly pine species (for a detailed study on the ecology and culture of this species, refer to [38]). To confirm this, we looked at the dominant species classification (as recorded by the FIA crew) for the 211 FIA plantation pine plots (as of 2009) in the entire region of ALS coverage (Figure 1). Approximately 94% of these plots were loblolly pine and 5% were longleaf pine (*Pinus palustris* Mill.).

To estimate site index, we used a dynamic site index equation based on a long-term loblolly pine plantation study that used many ( $n = 186$ ) permanent sample plots [39]. These plots adequately sampled the loblolly pine range stretching from Virginia (in the east) to Texas (in the west). The equation developed by that study is:

$$SI = \frac{85.75 + X_0}{1 + (4474/X_0) \times (ba)^{-1.107}} \quad (1)$$

where  $X_0$  is given by:

$$X_0 = \frac{1}{2}(dh - 85.75 + \sqrt{(dh - 85.75)^2 + 4 \times 4474 \times dh \times age^{-1.107}}) \quad (2)$$

where  $SI$  is site index (in feet),  $dh$  is dominant height (in feet),  $age$  is age of forest stand (years) and  $ba$  is base age (in years; 25 in our case). Site index estimated by Equation (1) is in feet, and we subsequently converted it to meters; all site index values reported by us henceforth are in meters using a base age of 25 years (unless specified otherwise). For site index estimation, we only considered stands that were at least 15 years of age, as such estimates are more reliable for such older stands (as the site index curves flatten out as age increases). Recall that every pixel inside a particular eVCT-delineated stand is given a single value of age, hence intra-stand variations in SI are purely due to height differences. The site index was calculated for each 0.09 ha ( $30 \times 30$  m) Landsat pixel inside these forest stands. The workflow for the generation of this map is shown in Figure 5.

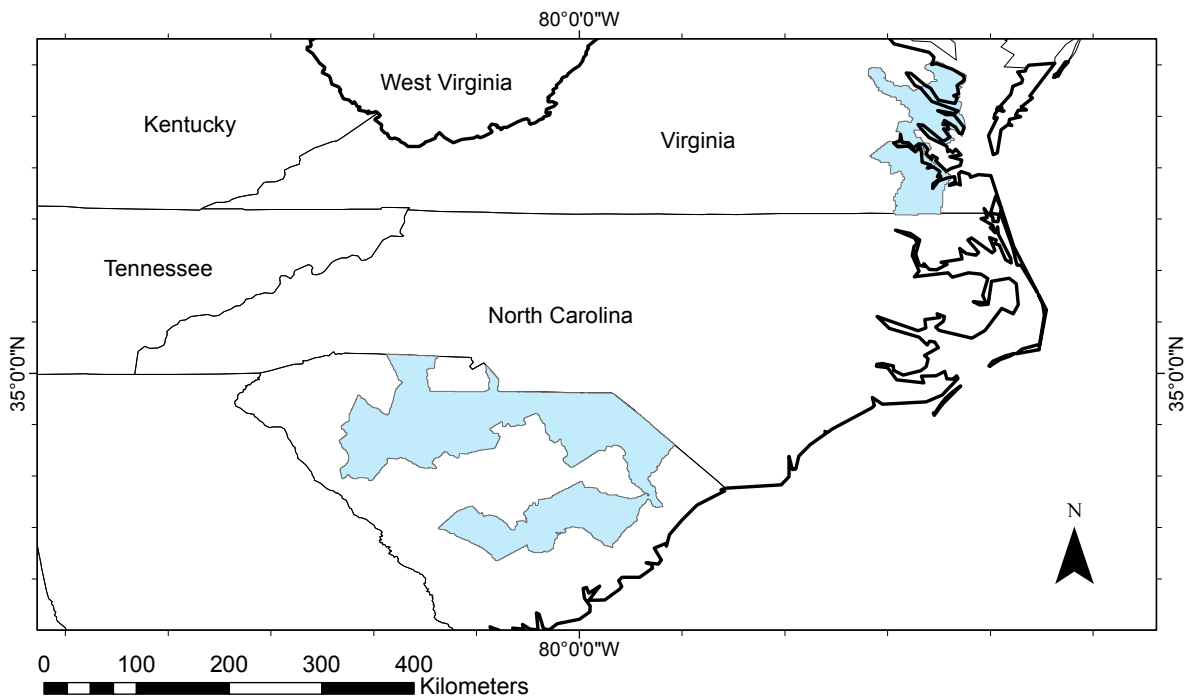


**Figure 4.** The extents of the two ALS projects over which the site index mapping was done are shown in blue shading. This represents an approximate area of 33,840 sq. km.

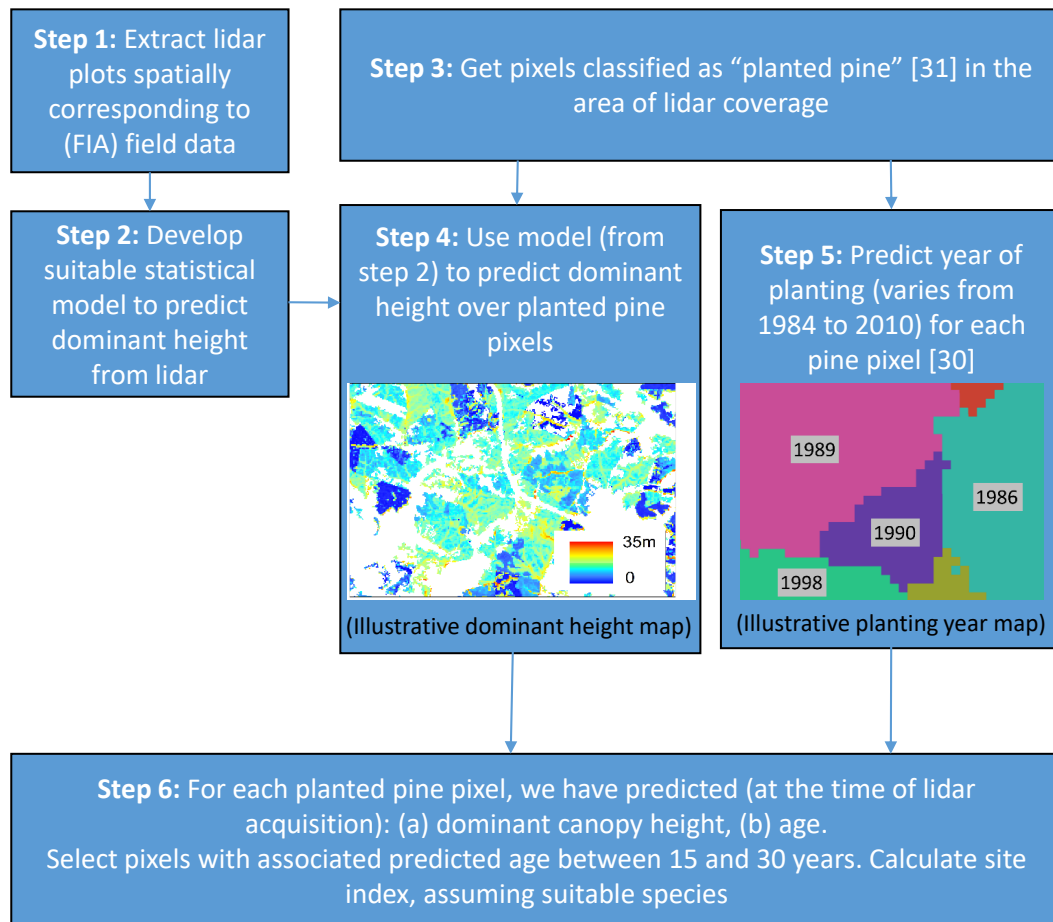


**Figure 5.** Major steps involved in the generation of the site index map.



### 2.5. Accuracy Assessment of Site Index Predictions

We used a Monte-Carlo approach to estimate the accuracy of the site index map. This method has been used in other remote-sensing based studies to propagate uncertainties in model input parameters [40]. This approach is popular when the output (site index, in our case) is a complex function of the inputs and when the distribution of the errors in the inputs are independently known or can be estimated.

In our case, the dynamic site index equation [39] states that:

$$\text{Site Index} = f(\text{Dominant height, age}) \quad (3)$$

The error distribution of the two right-hand-side components of Equation (3) are estimated in the following way:

1. Dominant height: This would be a normal distribution of mean 0.0 and standard deviation ( $\sigma$ ) equal to the root mean square error of the OLS-based linear model.
2. Age, predicted by eVCT: For this, we used the following independent ground-truth sources:
  - (a) Appomattox-Buckingham State Forest plot set: This is a set of 23 loblolly pine forest plots located in stands of known age in central Virginia, USA [41]. We have good estimates of the age of these stands, based on quality-checked planting records. However, these plots are relatively few in number and their coverage is geographically limited.
  - (b) FIA plot set: This is a set of 75 FIA plantation pine plots for which ages (year of planting) were available. The accuracy of these is variable, as the availability of planting records and reliable tree core data is limited. The lack of agreement between the FIA field estimates of age and eVCT is *assumed* to be due to erroneous eVCT ages. Note that this may not always be true, especially given the uncertainty in FIA age estimates.

The error distribution in the eVCT-based age was then estimated by randomly sampling among these plots, and getting the difference between the ages.

We performed 10,000 Monte-Carlo trials. For each such trial, a paired set of  $(\hat{y}_i, y_i)$  values were generated, where  $\hat{y}_i$  is the ALS-based site index prediction,  $y_i$  is the *estimated* reference value (obtained using the estimated error distributions above) and  $\bar{y}$  is the average of all generated reference values. The bias, the RMSE and the relative RMSE (%RMSE) were then calculated using standard formulas:

$$\text{bias} = \frac{1}{N} \sum_{i=1}^N (\hat{y}_i - y_i) \quad (4)$$

$$\text{RMSE} = \sqrt{\frac{1}{N} \sum_{i=1}^N (\hat{y}_i - y_i)^2} \quad (5)$$

$$\% \text{RMSE} = \frac{\text{RMSE} \times 100.0}{\bar{y}} \quad (6)$$

### 2.6. HU-Based Spatial Aggregation

We then spatially aggregated the pixel-level site index values to distinct hydrological units (corresponding to watersheds, henceforth HUs), a biophysically meaningful unit of aggregation for regional-level forest vegetation studies [42,43]. This was done by calculating the mean value of all sample points in an HU. Such aggregation also helps in better visualization, i.e., enabling the reader to visually discern distinct spatial trends (e.g., of the average SI per HUC) over the entire study area from the map. The 12-digit hydrologic unit (HUC-12) was the unit of aggregation used.

The spatial aggregation operation on the site index raster was done using 50,000 sample points, for better computational tractability. We also overlaid level two (L2) ecological regions from the US Environmental Policy Agency (EPA) [44] over the maps generated as they have been used previously to partially attribute measured plot-level differences in forest productivity [45,46]. There are two such ecological regions within our ALS coverage area; the EPA labels them as “Mississippi alluvial and Southeast USA coastal plains” (along the coast, henceforth referred to as “coastal plains”) and the “Southeastern USA plains” (in the interior, henceforth “southeastern plains”). The Kruskal–Wallis rank-based test was used to ascertain if the differences in means noticed at the HU level were statistically significant. Then, the Steel–Dwass all-pairs test (a non-parametric version of Tukey’s HSD test) was used to identify groups of HUs with such statistically significant differences in mean site index values. Both statistical tests were done using the 50,000 sample points mentioned above (each such point being labeled with the HU with which it is associated).

### 3. Results

#### 3.1. Canopy Height Model

We selected the 70th percentile of ALS heights ( $h_{70}$ ) as the independent variable for the regression model after examination of the correlation between plot-level ALS distributional metrics and dominant canopy heights. The correlation of  $h_{70}$  with dominant heights over all plots was 91.9%.

The linear regression model formulated has the form:

$$\text{Dominant height} = 0.90138 \times h_{70} + 4.2867 \quad (7)$$

The  $R^2$  of the fit was 0.84, the RMSE was 1.85 m and the bias was less than 0.0001 m. In addition,  $h_{70}$  was highly significant ( $p < 0.0001$ ). The scatterplot illustrating the fit can be seen in Figure 6.

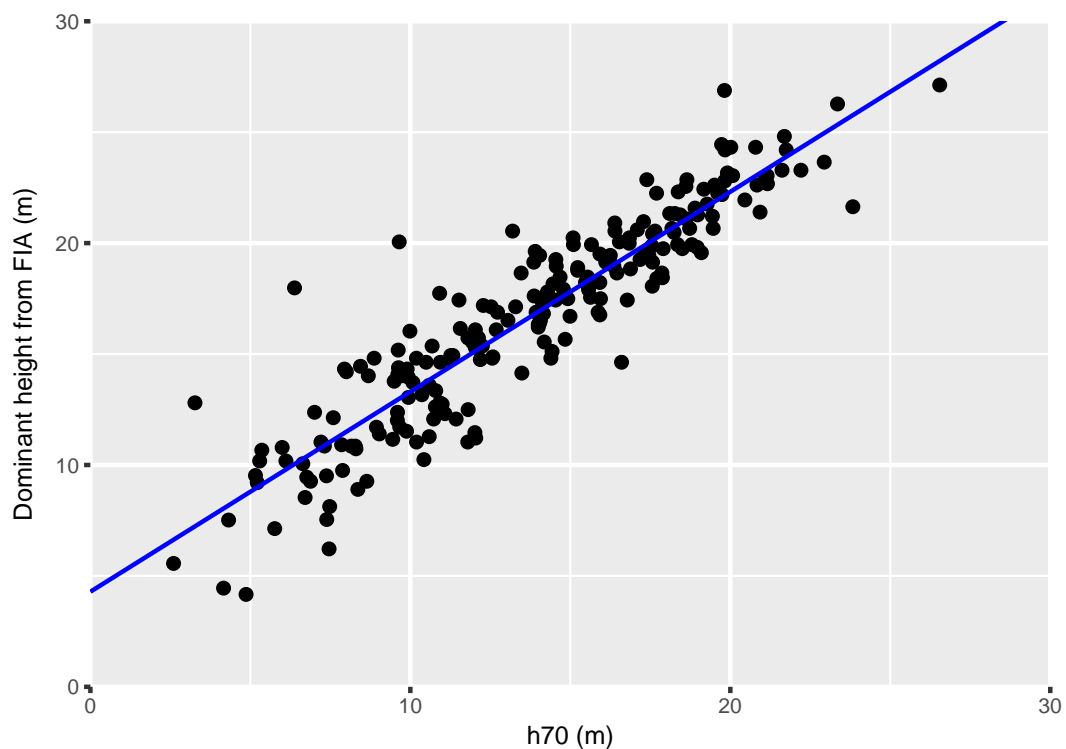


**Figure 6.** Scatterplot showing the plot-level agreement between the 70th percentile of ALS first return heights and the FIA-measured average dominant tree height ( $n = 211$  plots). The fitted linear model is indicated by the blue line.

### 3.2. Accuracy Assessment of Site Index Map

The accuracy of site index values generated was assessed using the methods outlined in Section 2.5. We used:

1. The Appomattox-Buckingham State Forest plot set: The bias of calculated site index was estimated to be  $-1.0$  m, the RMSE estimate was 3.0 m, and the relative RMSE was 15.1%.
2. FIA plot set: In this case, the estimated bias was  $-0.28$  m, the RMSE was 3.8 m, and the relative RMSE was 19.7%.

We generated a site index map as per the steps outlined in Section 2. A total of 22,027 plantation pine forest stands of ages between 15 and 27 years (at the time of ALS acquisition) were identified by the combination of eVCT [30] and Landsat-based pine stand identification algorithms [31]. The site index was predicted at the individual Landsat pixel level; that is, for a total loblolly pine forest area of approximately 832 sq. km. As the generated site index map is too large and too sparse for presentation in its entirety, we show a sample section in Newberry County, South Carolina (see Figure 7). The distribution of site index can be seen in Figure 8.

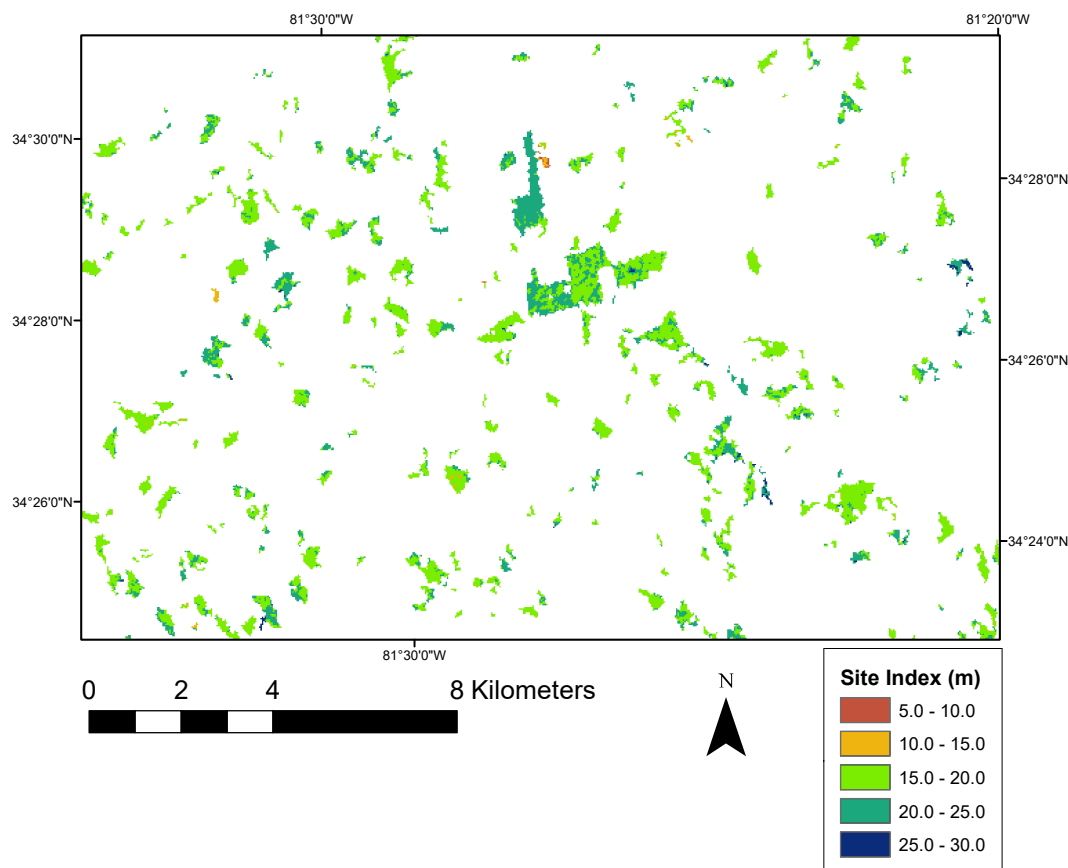


**Figure 7.** A part of the site index map generated is shown here at a scale where forest stands are visible (Newberry County, South Carolina). A very small percent of pixels (less than 0.1%) where site index values more than 30.0 m were predicted are not shown (as they were mostly model over-predictions). Most stands register reasonable to good site index values (e.g., greater than 20.0 m) while some under-perform (less than 10.0). However, the fairly large error in SI (RMSE of 3.0) should be kept in mind when performing such analysis at the individual pixel level.

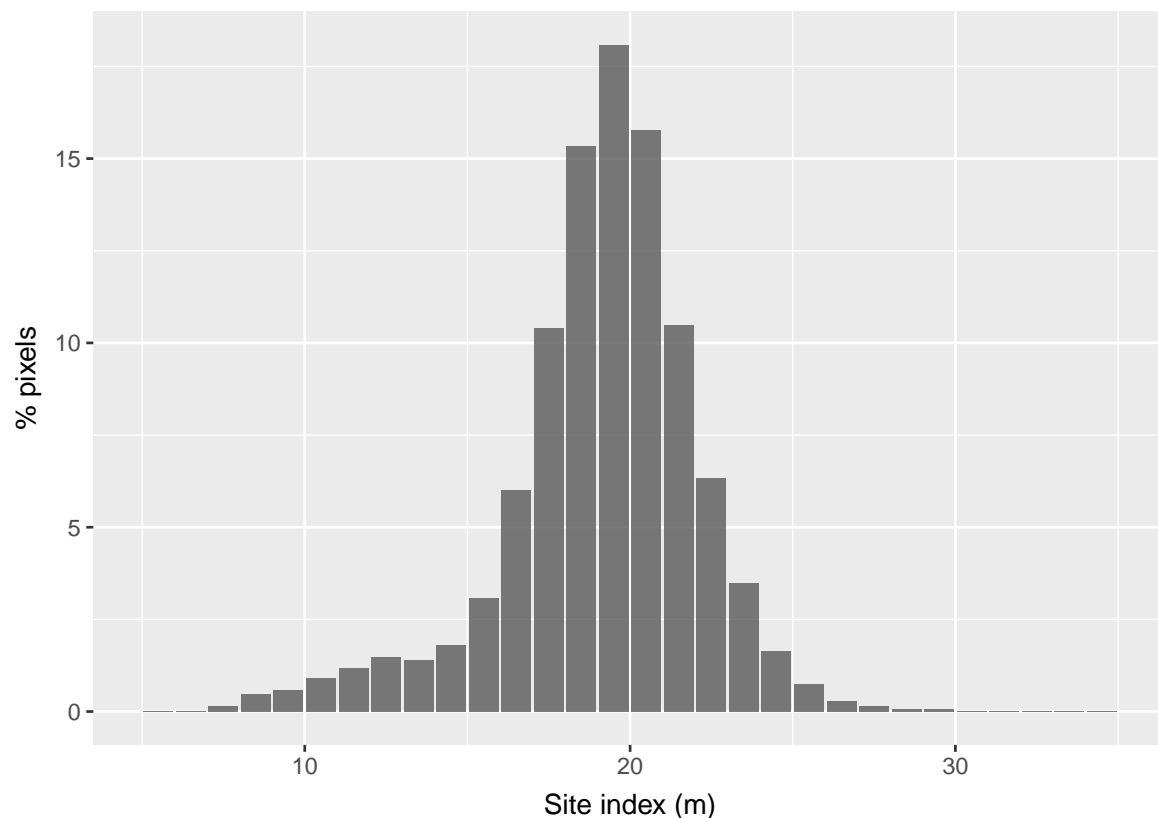


**Figure 8.** The distribution of site index values over the surveyed landscape (based on 50,000 sample points taken from the ALS coverage region of Figure 4). The site index distribution had a median value of 19.4 m, the 5th percentile value of 13.0 and the 95th percentile value of 23.3 m.

The point-level SI values were aggregated to the HU level (Figure 9). The Kruskal–Wallis test and the Steel–Dwass all-pairs test indicated that all pairs of HUs had statistically significant differences in their mean site index values. One can see in Figure 9 that most of the HUs had SI values between 15.1 and 26.0. A distinct divide can be noticed with respect to the ecoregions. That is, almost all the high site index HUs were in the coastal plains (near the eastern coast) while almost all the low site index HUs were on the west side of the study area, in the southeastern plains ecoregion. This may indicate that coastal plain soils and climatic conditions are better suited for loblolly pine growth. HUs that have lower site index seemed to cluster together, possibly indicating that their performance was more strongly linked to broad geographic reasons, rather than site-specific management ones.

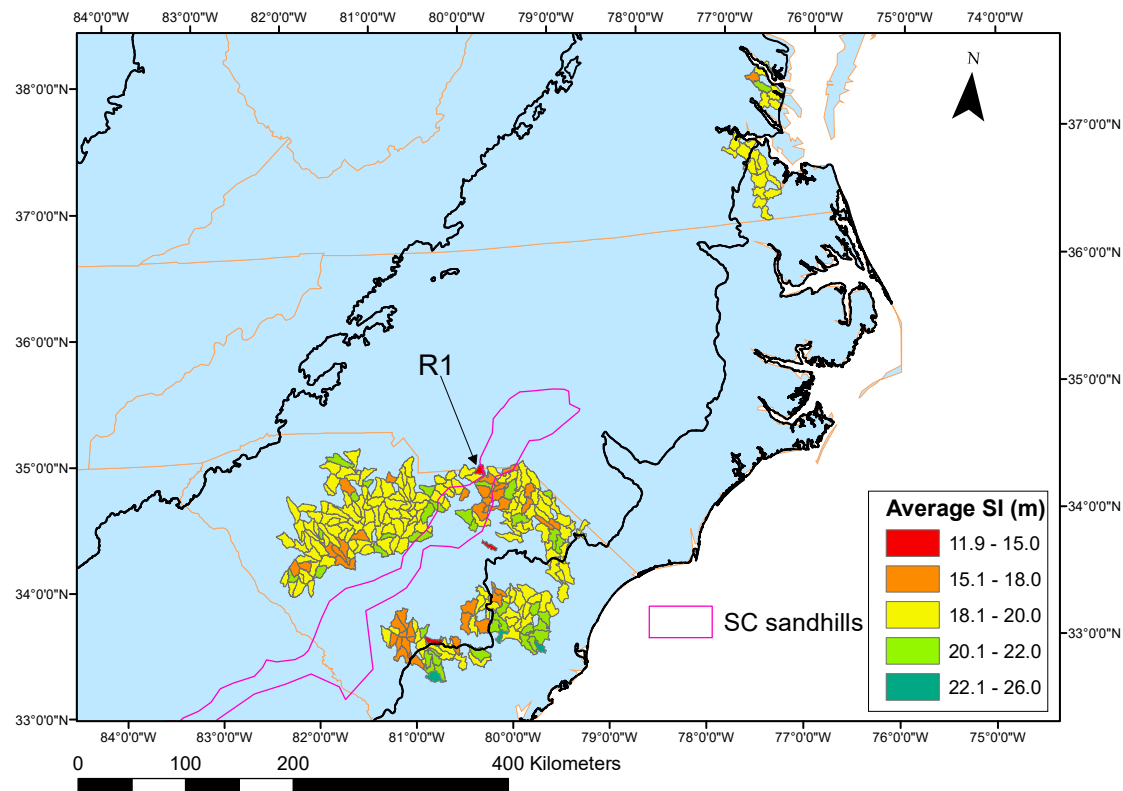


**Figure 9.** The average site index for all stands that fall in a given hydrological unit is depicted. Only hydrological units with at least 4.5 ha of surveyed forest stand area (50 pixels) are shown. The thick black lines demarcate EPA level 2 ecoregions (as per Omernik (1987) [44]), see text for more details. The polygon with the pink outline roughly demarcates the South Carolina sandhills region, where low productivity has been documented [47]. The general region pointed to by text “R1” in the map, i.e., the 6–7 HUCs with estimated low productivity (18.0 and lower) all seem to lie in this region. This seems to indicate that our ALS-based site index map can effectively identify regions of low productivity.

#### 4. Discussion

In this study, we combined various remote-sensing products to generate a planted pine site index map for large areas of the southeastern USA. The accuracy of the map is contingent on several factors: (1) the accuracy of the planted pine map used [31]; (2) the correctness of the assumption that all planted pine is loblolly pine; (3) the regional applicability of the site index equation form [39]; and (4) the accuracy of both the age and height estimations. The species assumption we made is that all plantation pine in Figure 4 area is loblolly pine. This is not the case; a small number of longleaf pine plantations are also present in that area (estimated to be around 5% by us). Nevertheless, these two species have similar growth patterns [48] and hence the errors associated with these assumptions are not expected to be large. Future refinements to the algorithm used for selecting planted pine may allow for selection of pure loblolly pine pixels.

Although the site index equation used here was from a study covering much of the native range of loblolly pine and age classes [39], it may not be representative for some forest stands. An alternative way to make site index predictions is the *guide curve method* [21], where a one-time measurement of a large sample of trees is used to construct a site index model. Our methods are more similar to those of Wulder et al. [20] where prior site index equations (for specified species) were applied to ALS predictions of stand height and inventory-based stand ages. Another study which is similar to us

(but involving a smaller area) is Noordermeer et al. [49] where two different methods for site index estimation are presented, given bitemporal ALS data: (1) by regressing field observations of SI with ALS-derived canopy height metrics; and (2) by selecting the site index curve that best explains the observed (bitemporal) difference in dominant heights.

In the rest of this section, we revisit our two research questions and discuss several caveats associated with them. We also explore some additional uses of our site index maps.

#### 4.1. Efficacy of Site Index Maps Based on Disparate ALS Projects Data and Landsat

Our site index estimates are minimally biased (Section 3.2) with an accuracy consistent with other similar approaches. This affirms that one can use low pulse density ALS data from disparate projects combined with Landsat-based age maps to reasonably predict site index over large areas. Our accuracy estimates compare favorably with levels reported by Tompaski et al. [21] (bias = 0.7 m, RMSE = 5.5 m, base age = 32 years), who used similar remote sensing data sources for site index prediction. Figure 6 shows that dominant heights could be well-predicted from ALS data, which contributed to overall stronger models.

Site index predictions are sensitive to errors in associated predictions of forest stand age. To further understand and quantify this in our case, we analyzed the agreement of forest stand age estimates (predicted by eVCT using remote sensing techniques) to those based on planting records or field visits (Figure 10). Age predictions of eVCT were found to be relatively unbiased, which partly explains the low bias of our site index predictions. The absolute age bias of approximately 1.1 years in both cases shown in Figure 10 is similar to the bias of 2.2 years reported by Tompalski et al. [21], who used fixed *disturbance index* thresholds to detect stand-clearing disturbances from Landsat time-series maps (and age was deduced). In Figure 10b, one can notice that many plots were assigned an age of either 24 or 26 years. This is to be expected, considering the following: (1) 1984 was when Landsat 5 data became available, and, as such, is the beginning of the VCT time series; and (2) as a result of some design considerations, VCT tends to assign high disturbance magnitudes at the beginning of the analyzed time series in some instances [33]. This translated into clearcuts being over-detected during 1984. Nevertheless, as time advances, there would be fewer and fewer planted pine stands that were last harvested in 1985, 1984 or earlier, thus the ability for eVCT or other techniques to estimate age is expected to increase. In the case of FIA data (Figure 10b), spurious age relationships seen are probably a product of eVCT errors (some caused by the VCT algorithm itself and some by the inherent noise found in Landsat data), imprecise FIA plot coordinates and inaccurate FIA age estimates. Because neither the FIA coordinates, age estimates nor eVCT have measures of error associated with them, it is difficult to parse out the main driver of the discrepancy.

We further looked at a small set of planted pine plots ( $n = 19$ ) where both site index predictions from ALS and field based site index estimates from FIA were available (Figure 11). The  $R^2$  of the fit was low: 1.8%. Similar regressions of ALS-derived site index with values from forest inventories have produced either low (0.03 in [20]) or moderate (0.42 in [19])  $R^2$  values. Nevertheless, in our case, if one considers only field plots where both age estimates are within  $\pm 5$  years in Figure 11 ( $n = 12$ ), the  $R^2$  of the fit improved to 46%; similarly for  $\pm 3$  years ( $n = 9$ ), the  $R^2$  was 77.5%. This can be seen in Figure 11, where plots with similar age estimates (from eVCT and FIA) tend to be near the 1:1 line, which shows that age discrepancies are likely a major cause of the overall lack of fit. Over-detection of disturbances in 1984 (see discussion above) is clearly responsible for many age discrepancies. Other likely causes have to be further investigated. Figure 11 also implies that dominant heights are well-predicted from ALS data. This is in agreement with previous literature indicating that ALS estimates of plot-level height metrics are accurate [27,50–52].

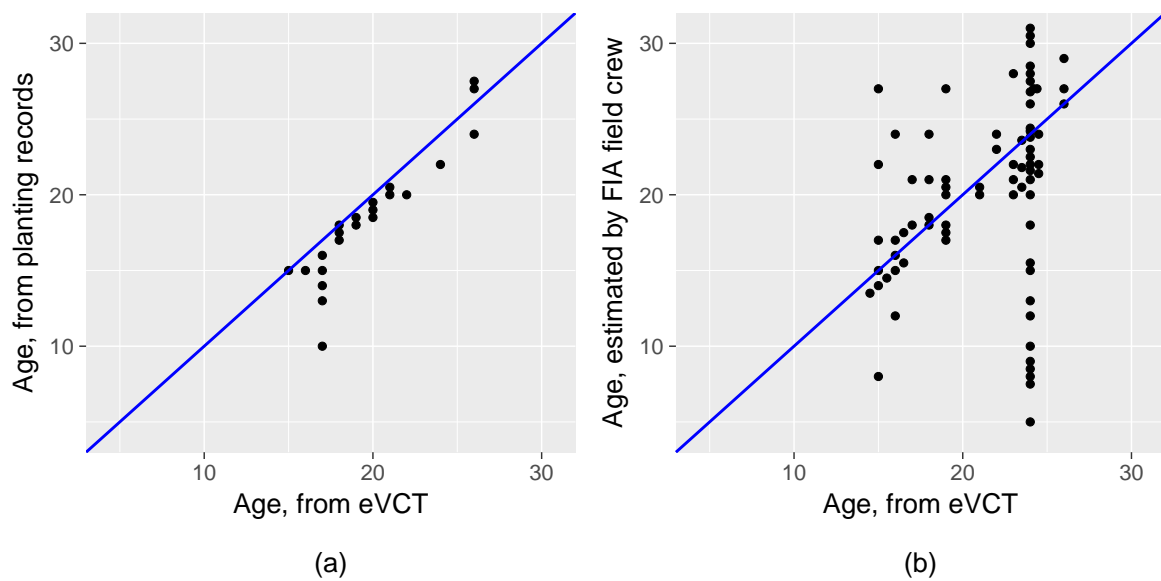


**Figure 10.** Correspondence between forest stand ages predicted by eVCT and estimated from other ground-truth sources (all ages are in years). The 1:1 line is shown in blue. Only plots that were indicated by eVCT to be 15 years of age or above were examined. Some points in the plot have been slightly jittered ( $\leq 0.5$  years) so that points do not lie on top of each other. (a) Age agreement, using quality-adjusted planting record data from the Appomattox-Buckingham State Forest plot set (23 plots, see Section 2.5). One extreme outlier point at  $(x, y) = (10, 72)$  is excluded. It can be seen that most points are near the 1:1 line. The bias is  $-1.1$  years. Around 87% of plots have  $\pm 3$  years age agreement while 91.3% of plots have  $\pm 5$  years, (b) Age agreement, using the set of 75 FIA plots. The pronounced “vertical line” of points corresponding to eVCT age = 24 is most likely due to VCT being less reliable at the beginning of the time series, see text for more details. The overall agreement is much weaker in this case. The bias is rather small (1.1 years). Around 65.3% of plots have  $\pm 3$  years age agreement, 73.3% of plots have  $\pm 5$  years and 85.3% have  $\pm 8$  years.

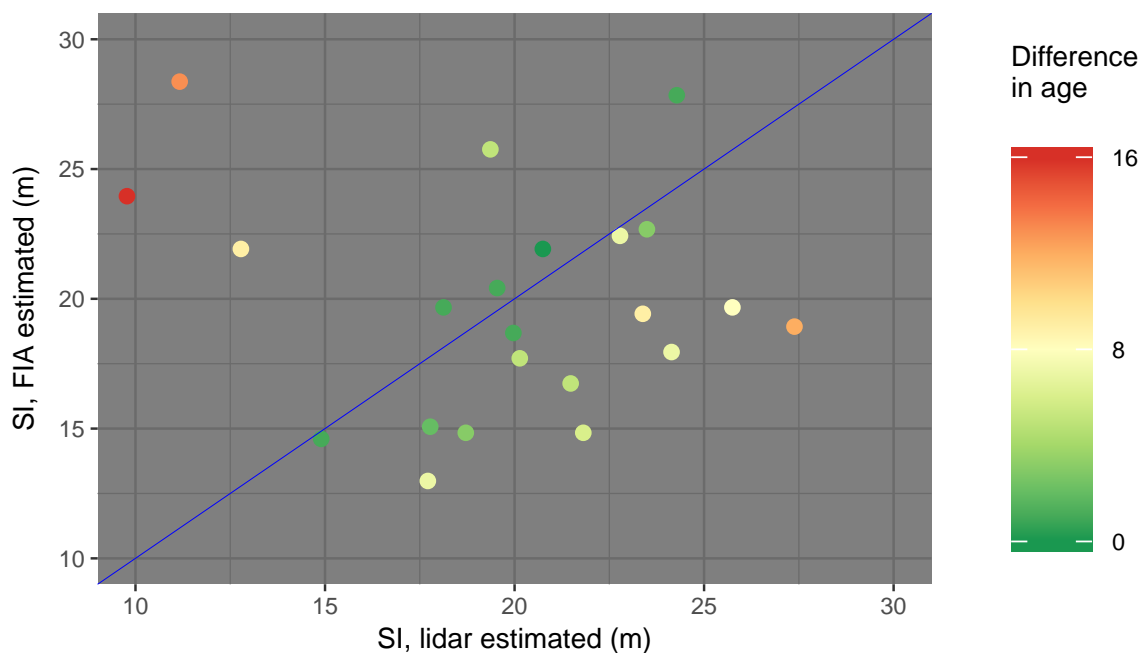


**Figure 11.** Correspondence between site index predictions from ALS and estimates from FIA for 19 planted pine plots. The absolute difference in age (years) predicted by eVCT and estimated by FIA is also indicated. The 1:1 line is shown in blue.

#### 4.2. Distribution and Regional Patterns of Productivity

It is forecast that the area of planted pine land use in southeastern US could more than double in the next 40 years. That is, it is expected to grow from 19% of the total forest area (thus, from 16 million ha of planted pine in 2010) to between 24% and 36% by 2060 [12], which highlights the relevance of this research. In Section 3, we outline the distribution and broad aggregated spatial pattern of current site productivity over large areas of this region. Confidence in our productivity estimates are further increased by the fact that the broad spatial trends of site index seen in Figure 9 are quite similar to a region-wide site index map derived from a biophysical model, as illustrated in [16] (see Figure 3d in that article). Further work is needed wherein HUs registering low site index in Figure 9 should be investigated and considered for possible management and policy interventions. For example, macronutrient addition has been found to be widely effective; a large and consistent growth increase (around 25%) after mid-rotation fertilization with nitrogen and phosphorous has been reported on the majority of soil types [53]. Deficiencies of other nutrients such as potassium, calcium, copper and boron have also been implicated [54]. Other soil-related issues pertinent to pine plantations such as texture, compaction, soil aeration and moisture and pH value [55] may be harder to address. This may be the reason Zhao et al. [11] reported that as much as 26% of plots was found to have poor response to treatments (such as nutrient additions) on a regional level. Nevertheless, there seems to be ample scope for additional management interventions in the region; for example, it was reported by Han et al. [5] that the percent of regional total greenhouse gas emission sequestered by forests in 11 southeast states could be increased from 13% to 23% through proper policies and using best land management practices.

#### 4.3. Contrasting Current and Historical Site Index Levels

An interesting question that arises in the context of our estimated site index distribution is whether it can be contrasted to historical estimates, and whether significant productivity changes can be detected over the large spatial scales analyzed. To address this question, we obtained historical loblolly pine site index values for the region from the USDA Natural Resource Conservation Service's Soil Survey Geographic Database (henceforth, SSURGO) [56]. These data were originally collected by first defining small-scale soil polygons over the whole landscape and then defining a good representative pine site index value for each such polygon (for base age of 50 years). As these data were mostly collected in the 1960s and 1970s, they are a good representation of the site index that had prevailed during those times. Loblolly pine site index was converted from base age 50 to 25 by using the base age invariant site index model developed by Dieguez-Aranda et al. [39]. We then estimated the change in site index over the region over the past four decades by subtracting the SSURGO site index from the ALS-predicted site index (at each of the 50,000 sample points mentioned in Section 2.6). The result of such a subtraction should be viewed with discretion, as we elaborate below. Nevertheless, a similar comparison of present-day SI values with historical SSURGO has been described in [26]. We aggregated differences in site index to the HU level, as before (Figure 12). The Kruskal–Wallis test and the Steel–Dwass all-pairs test were again used to confirm that there were significant differences between all pairs of HUs.

A histogram of the difference between ALS predicted loblolly pine site index and SSURGO estimated site index is shown in Figure 13. A general increase in site index is noticed for the whole region, which could be mostly attributed to management interventions [11,53], although the increase in carbon dioxide concentrations [43,57,58], temperature and nitrogen deposition [59] may be factors. Our estimates of the region-wide increase in site index compare well to a similar estimate by Subedi et al. [60]. In that article, the authors compared the current site index value with that of SSURGO-based values for various loblolly pine stands across 21 study sites, spanning the geographic breadth of the Southeast. They found that site index had increased by around 5–7 m (on average) on these stands. This compares well with the increase that we observed over the whole region (mean = 2.8 m, median = 3.2 m, see Figure 13). Further, it should be noted that we estimated a negative



bias of approximately 0.3–0.7 m for our site index prediction method (see Section 3.2), which means that the actual increase could be closer to 3.5 m.

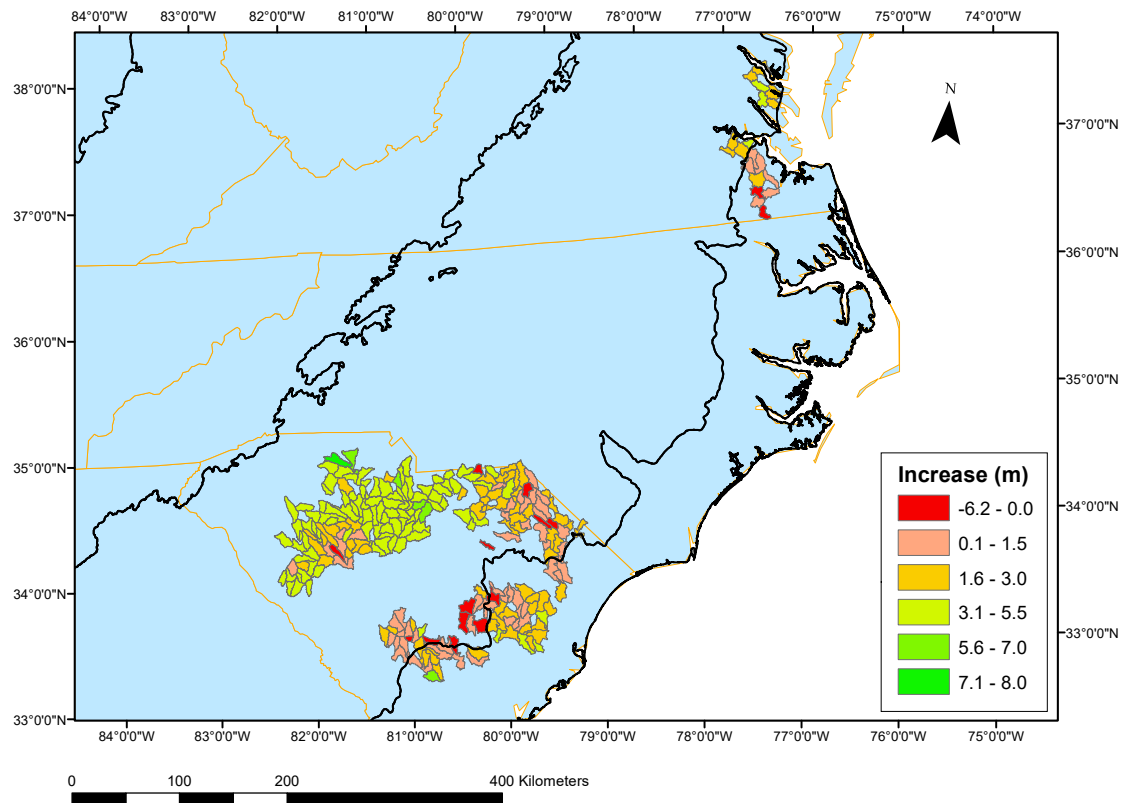


**Figure 12.** The average site index difference (between lidar-based and historical SSURGO estimates) for stands that fall in the hydrological unit is shown. Only hydrological units with at least 4.5 ha of surveyed forest stand area (50 pixels) are considered. The thick black lines here demarcate ecoregions (EPA level 2 ecoregions as per Omernik 1987 [44]), see text for more details.

Nevertheless, it should be noted that different methods were used for estimation of SI, in the case of our effort and that of SSURGO. Hence, these comparisons contain uncertainties that are unaccounted for and hence should be viewed and analyzed with caution. However, a similar comparison was reported by Ham et al. [26], who found both lidar-derived and inventory-based modern-day site index (i.e., of approximately 2010) to be significantly different from SSURGO (higher in almost all cases). A strong trend of large productivity increases in the western interior parts can be seen in South Carolina (Figure 12); this seems to indicate that management interventions may have been most effective on the poorer soils of those interior regions. In addition, around 16% of our sample points registered a decrease in site index over the years. A similar phenomenon has been reported by Zhao et al. [11] where they report that as much as 26% of the 850 plots surveyed had a near-zero or negative increase in site index.

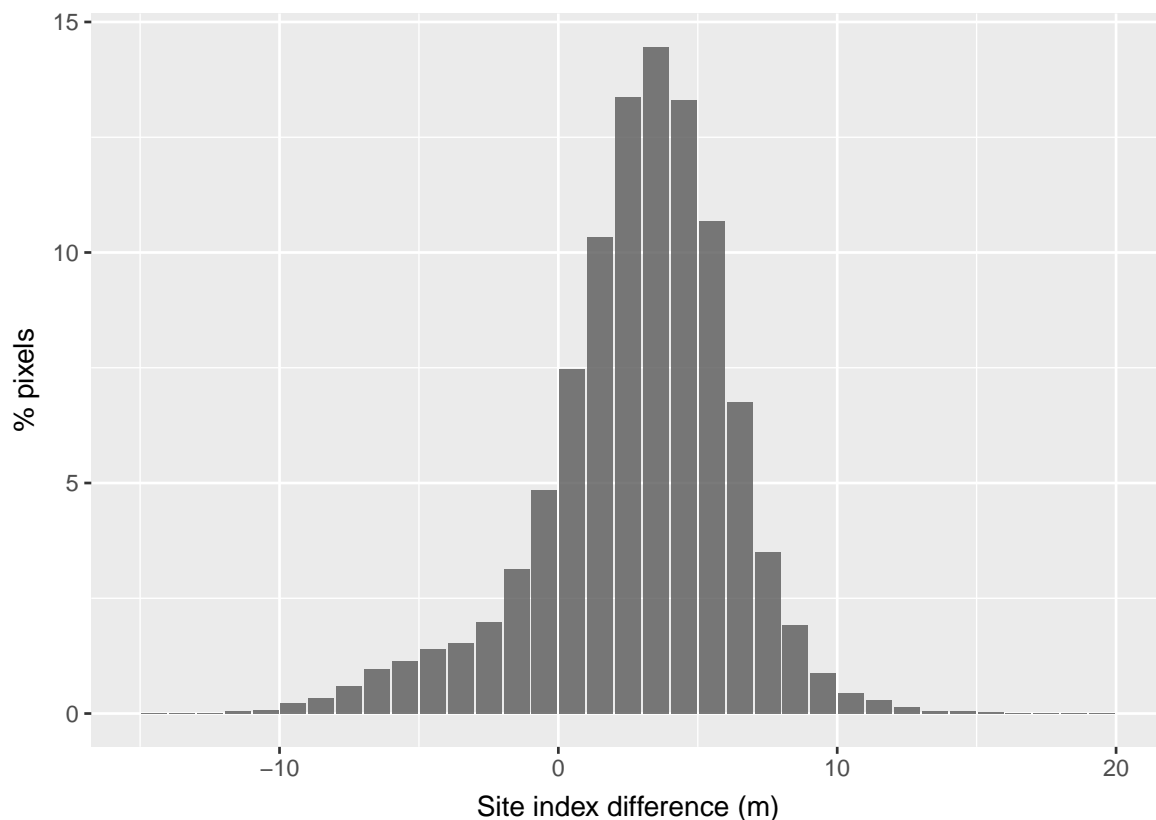


**Figure 13.** The difference between ALS-predicted site index (as of 2008 and 2010) and SSURGO-estimated site index (around the 1970s). Histogram mean = 2.8 m, median = 3.2 m.

#### 4.4. Forest Productivity Maps: Other Utilization Avenues

Some possible alternate uses of productivity maps (such as ours) warrant mention at this point. These estimates could be used to deduce the intensity of management for specific sites. Again, the modeling community could also benefit from such site index maps: two classes of models that could be better calibrated and validated with such maps are forest productivity models and regional wood supply models. For example, Subedi et al. [60] pointed to a mechanism by which stand-level forest productivity could be predicted (and updated for changing climate conditions and management regimes) for loblolly pine stands on a regional scale. They proposed a method by which SSURGO-based soil fertility rating could be used as input to  $3PG_{lob}$ , a loblolly pine productivity model. Our site index predictions would be useful as validating reference data for such efforts. Recently, there have been promising efforts in the direction of model-data assimilation for ecological forecasting [16]. In general terms, our remote sensed productivity estimates could contribute as “proxy” observational data, in such contexts.

The results of this study have the following implications: (1) ALS acquired via disparate projects for mostly non-forestry purposes (such as topographic mapping) can be used to generate planted pine dominant height maps over large areas, (2) Such maps can be combined with stand age derived from Landsat-based land-cover tracking algorithms, enabling periodic assessment of site index trends for large areas, especially given that site index is a dynamic quantity and may need such updates [20], and (3) A large proportion of planted pine forests in southeastern United States has low site index and may have a sizable potential for additional carbon sequestration through better management interventions. Moreover, we hypothesize that pine site index seems to have largely increased in the region, with considerable differences between historical (1960 and 1970s) and recent (circa 2010) productivity estimated. The magnitude of this calculated increase is higher towards the interior regions.

## 5. Conclusions

In this study, we presented and evaluated a method to generate site index estimates over large areas in the southeastern U.S., an important region with respect to carbon sequestration and forest plantation activity. Our method generates productivity maps only over relatively young pine plantations established after 1984, due to constraints in age-related remote sensing products. The error associated with these estimates were shown to be comparable to similar approaches, hence the site index maps generated provide a realistic picture of the broad spatial trends of productivity over the region. Several areas were identified as having low productivity in Virginia and South Carolina, which might have important ramifications for land-use policy makers and forest managers. Further research aimed at understanding the observed spatial patterns of pine productivity could lead to important insights pertaining to forest ecology and socio-economics of forest management practices.

**Author Contributions:** R.G., V.A.T. and R.H.W. conceived and designed the research experiments, with inputs from J.S.K., M.E.F., J.W.C. and T.R.F.; software was written by R.G.; auxiliary datasets were provided by J.S.K and M.E.F; validation data was compiled by R.G. and J.W.C.; validation data was also obtained by V.F.Q.; analysis was done by R.G. with contributions from J.W.C., V.A.T. and R.H.W.; writing—original draft preparation, R.G.; all the authors contributed to writing—review and editing.

**Funding:** This work was funded by the PINEMAP project (<http://pinemap.org>) sponsored by the USDA's National Institute of Food and Agriculture (NIFA). We would also like to acknowledge the US Department of Agriculture (USDA) McIntire-Stennis Formula Grant.

**Conflicts of Interest:** The authors declare no conflict of interest.

## References

1. Coops, N.C. Characterizing forest growth and productivity using remotely sensed data. *Curr. For. Rep.* **2015**, *1*, 195–205. [[CrossRef](#)]
2. Splachtn, B.E. Height growth and site index models for Pacific silver fir in southwestern British Columbia. *J. Ecosyst. Manag.* **2001**, *1*, 1–14.
3. Dyck, B. Precision forestry—The path to increased profitability. In Proceedings of the 2nd International Precision Forestry Symposium, Seattle, WA, USA, 15–17 June 2003; pp. 3–8.
4. Turner, D.P.; Koerper, G.J.; Harmon, M.E.; Lee, J.J. A carbon budget for forests of the conterminous United States. *Ecol. Appl.* **1995**, *5*, 421–436. [[CrossRef](#)]
5. Han, F.X.; Plodinec, M.J.; Su, Y.; Monts, D.L.; Li, Z. Terrestrial carbon pools in southeast and south-central United States. *Clim. Chang.* **2007**, *84*, 191–202. [[CrossRef](#)]
6. USFS. *Future of America's Forest and Rangelands: Forest Service 2010 Resources Planning Act Assessment*; General Technical Report GTR-WO-87; USDA Forest Service: Washington, DC, USA, 2012.
7. Skovsgaard, J.P.; Vanclay, J.K. Forest site productivity: A review of the evolution of dendrometric concepts for even-aged stands. *Forestry* **2008**, *81*, 13–31. [[CrossRef](#)]
8. Sellers, P.J.; Shuttleworth, W.J.; Dorman, J.L.; Dalcher, A.; Roberts, J.M. Calibrating the simple biosphere model for Amazonian tropical forest using field and remote sensing data. Part I: Average calibration with field data. *J. Appl. Meteorol.* **1989**, *28*, 727–759. [[CrossRef](#)]
9. Launay, M.; Guerif, M. Assimilating remote sensing data into a crop model to improve predictive performance for spatial applications. *Agric. Ecosyst. Environ.* **2005**, *111*, 321–339. [[CrossRef](#)]
10. Avery, T.E.; Burkhart, H.E. *Forest Measurements*; Waveland Press: Long Grove, IL, USA, 2015.
11. Zhao, D.; Kane, M.; Teskey, R.; Fox, T.R.; Albaugh, T.J.; Allen, H.L.; Rubilar, R. Maximum response of loblolly pine plantations to silvicultural management in the southern United States. *For. Ecol. Manag.* **2016**, *375*, 105–111. [[CrossRef](#)]
12. Wear, D.; Greis, J. *The Southern Forest Futures Project: Summary Report*; Technical Report SRS-GTR-168; USDA-Forest Service, Southern Research Station: Asheville, NC, USA, 2012.
13. Sabatia, C.O.; Burkhart, H.E. Predicting site index of plantation loblolly pine from biophysical variables. *For. Ecol. Manag.* **2014**, *326*, 142–156. [[CrossRef](#)]
14. Bryars, C.; Maier, C.; Zhao, D.; Kane, M.; Borders, B.; Will, R.; Teskey, R. Fixed physiological parameters in the 3-PG model produced accurate estimates of loblolly pine growth on sites in different geographic regions. *For. Ecol. Manag.* **2013**, *289*, 501–514. [[CrossRef](#)]

15. Carlson, C.A.; Fox, T.R.; Creighton, J.; Dougherty, P.M.; Johnson, J.R. Nine-year growth responses to planting density manipulation and repeated early fertilization in a loblolly pine stand in the Virginia Piedmont. *South. J. Appl. For.* **2009**, *33*, 109–114.
16. Thomas, R.Q.; Brooks, E.B.; Jersild, A.L.; Ward, E.J.; Wynne, R.H.; Albaugh, T.J.; Dinon-Aldridge, H.; Burkhart, H.E.; Domec, J.C.; Fox, T.R. Leveraging 35 years of *Pinus taeda* research in the southeastern US to constrain forest carbon cycle predictions: Regional data assimilation using ecosystem experiments. *Biogeosciences* **2017**, *14*, 3525. [[CrossRef](#)]
17. Jokela, E.J.; Dougherty, P.M.; Martin, T.A. Production dynamics of intensively managed loblolly pine stands in the southern United States: A synthesis of seven long-term experiments. *For. Ecol. Manag.* **2004**, *192*, 117–130. [[CrossRef](#)]
18. Miller, J.H.; Zutter, B.R.; Zedaker, S.M.; Edwards, M.B.; Newbold, R.A. Growth and yield relative to competition for loblolly pine plantations to midrotation: A southeastern United States regional study. *South. J. Appl. For.* **2003**, *27*, 237–252.
19. Gatzliolis, D. LiDAR-derived site index in the US Pacific Northwest: Challenges and opportunities. In Proceedings of the ISPRS Workshop on Laser Scanning 2007 and SilviLaser 2007, Espoo, Finland, 12–14 September 2007.
20. Wulder, M.A.; White, J.C.; Stinson, G.; Hilker, T.; Kurz, W.A.; Coops, N.C.; St-Onge, B.; Trofymow, J.T. Implications of differing input data sources and approaches upon forest carbon stock estimation. *Environ. Monit. Assess.* **2010**, *166*, 543–561. [[CrossRef](#)] [[PubMed](#)]
21. Tompalski, P.; Coops, N.C.; White, J.C.; Wulder, M.A.; Pickell, P.D. Estimating forest site productivity using airborne laser scanning data and Landsat time series. *Can. J. Remote Sens.* **2015**, *41*, 232–245. [[CrossRef](#)]
22. Kandare, K.; Ørka, H.O.; Dalponte, M.; Næsset, E.; Gobakken, T. Individual tree crown approach for predicting site index in boreal forests using airborne laser scanning and hyperspectral data. *Int. J. Appl. Earth Obs. Geoinf.* **2017**, *60*, 72–82. [[CrossRef](#)]
23. Packalén, P.; Mehtätalo, L.; Maltamo, M. ALS-based estimation of plot volume and site index in a eucalyptus plantation with a nonlinear mixed-effect model that accounts for the clone effect. *Ann. For. Sci.* **2011**, *68*, 1085. [[CrossRef](#)]
24. Watt, M.S.; Dash, J.P.; Bhandari, S.; Watt, P. Comparing parametric and non-parametric methods of predicting Site Index for radiata pine using combinations of data derived from environmental surfaces, satellite imagery and airborne laser scanning. *For. Ecol. Manag.* **2015**, *357*, 1–9. [[CrossRef](#)]
25. Socha, J.; Pierzchalski, M.; Bałazy, R.; Ciesielski, M. Modelling top height growth and site index using repeated laser scanning data. *For. Ecol. Manag.* **2017**, *406*, 307–317. [[CrossRef](#)]
26. Ham, S.A.; Mikhailova, E.A.; Gering, L.R.; Post, C.J.; Bridges, W.C.; Cox, S.K. Temporal analysis of field, SSURGO, and LiDAR-derived site indices in the southeastern United States. *Soil Sci.* **2013**, *178*, 325–334. [[CrossRef](#)]
27. Gopalakrishnan, R.; Thomas, V.A.; Coulston, J.W.; Wynne, R.H. Prediction of canopy heights over a large region using heterogeneous lidar datasets: Efficacy and challenges. *Remote Sens.* **2015**, *7*, 11036–11060. [[CrossRef](#)]
28. Sexton, J.O.; Bax, T.; Siqueira, P.; Swenson, J.J.; Hensley, S. A comparison of lidar, radar, and field measurements of canopy height in pine and hardwood forests of southeastern North America. *For. Ecol. Manag.* **2009**, *257*, 1136–1147. [[CrossRef](#)]
29. Popescu, S.C.; Wynne, R.H. Seeing the trees in the forest: Using lidar and multispectral data fusion with local filtering and variable window size for estimating tree height. *Photogramm. Eng. Remote Sens.* **2004**, *70*, 589–604. [[CrossRef](#)]
30. Kauffman, J.S.; Prisley, S.P. Automated estimation of forest stand age using Vegetation Change Tracker and machine learning. *Math. Comput. For. Nat. Resour. Sci.* **2016**, *8*, 4.
31. Fagan, M.E.; Morton, D.C.; Cook, B.D.; Masek, J.; Zhao, F.; Nelson, R.F.; Huang, C. Mapping pine plantations in the southeastern US using structural, spectral, and temporal remote sensing data. *Remote Sens. Environ.* **2018**, *216*, 415–426. [[CrossRef](#)]
32. Sugarbaker, L.J.; Constance, E.W.; Heidemann, H.K.; Jason, A.L.; Lukas Vicki, S.D.; Stoker, J.M. *The 3D Elevation Program Initiative: A Call for Action*; US Geological Survey: Reston, VA, USA, 2014.

33. Huang, C.; Goward, S.N.; Masek, J.G.; Thomas, N.; Zhu, Z.; Vogelmann, J.E. An automated approach for reconstructing recent forest disturbance history using dense Landsat time series stacks. *Remote Sens. Environ.* **2010**, *114*, 183–198. [[CrossRef](#)]
34. Hansen, M.C.; Potapov, P.V.; Moore, R.; Hancher, M.; Turubanova, S.A.; Tyukavina, A.; Thau, D.; Stehman, S.V.; Goetz, S.J.; Loveland, T.R. High-resolution global maps of 21st-century forest cover change. *Science* **2013**, *342*, 850–853. [[CrossRef](#)] [[PubMed](#)]
35. Bechtold, W.A.; Patterson, P.L. *The Enhanced Forest Inventory and Analysis Program: National Sampling Design and Estimation Procedures*; US Department of Agriculture Forest Service, Southern Research Station: Asheville, NC, USA, 2005.
36. McRoberts, R.E. The effects of rectification and Global Positioning System errors on satellite image-based estimates of forest area. *Remote Sens. Environ.* **2010**, *114*, 1710–1717. [[CrossRef](#)]
37. White, J.C.; Wulder, M.A.; Vastaranta, M.; Coops, N.C.; Pitt, D.; Woods, M. The utility of image-based point clouds for forest inventory: A comparison with airborne laser scanning. *Forests* **2013**, *4*, 518–536. [[CrossRef](#)]
38. Schultz, R.P. *Loblolly Pine: The Ecology and Culture of Loblolly Pine (Pinus taeda L.)*; Department of Agriculture, Forest Service: Washington, DC, USA, 1997.
39. Diéguez-Aranda, U.; Burkhart, H.E.; Amateis, R.L. Dynamic site model for loblolly pine (*Pinus taeda* L.) plantations in the United States. *For. Sci.* **2006**, *52*, 262–272.
40. Lobell, D.B.; Asner, G.P.; Ortiz-Monasterio, J.I.; Benning, T.L. Remote sensing of regional crop production in the Yaqui Valley, Mexico: Estimates and uncertainties. *Agric. Ecosyst. Environ.* **2003**, *94*, 205–220. [[CrossRef](#)]
41. Quirino, V.F. Evaluating the Potential for Estimating Age of Even-Aged Loblolly Pine Stands Using Active and Passive Remote Sensing Data. Ph.D. Dissertation, Virginia Tech., Blacksburg, VA, USA, 2014.
42. Seaber, P.R.; Kapinos, F.P.; Knapp, G.L. *Hydrologic Unit Maps*; US Government Printing Office: Denver, CO, USA, 1987.
43. Burkhart, H.E.; Brooks, E.B.; Dinon-Aldridge, H.; Sabatia, C.O.; Gyawali, N.; Wynne, R.H.; Thomas, V.A. Regional Simulations of Loblolly Pine Productivity with CO<sub>2</sub> Enrichment and Changing Climate Scenarios. *For. Sci.* **2018**, *64*, 349–357. [[CrossRef](#)]
44. Omernik, J.M. Ecoregions of the conterminous United States. *Ann. Assoc. Am. Geogr.* **1987**, *77*, 118–125. [[CrossRef](#)]
45. Belote, R.T.; Priskey, S.; Jones, R.H.; Fitzpatrick, M.; de Beurs, K. Forest productivity and tree diversity relationships depend on ecological context within mid-Atlantic and Appalachian forests (USA). *For. Ecol. Manag.* **2011**, *261*, 1315–1324. [[CrossRef](#)]
46. Noormets, A.; Gavazzi, M.J.; McNulty, S.G.; Domec, J.C.; Sun, G.E.; King, J.S.; Chen, J. Response of carbon fluxes to drought in a coastal plain loblolly pine forest. *Glob. Chang. Biol.* **2010**, *16*, 272–287. [[CrossRef](#)]
47. NRCS. *Land Resource Regions and Major Land Resource Areas of the United States, the Caribbean, and the Pacific Basin*; US Department of Agriculture Handbook: Washington, DC, USA, 2006.
48. Carmean, W.H.; Hahn, J.T.; Jacobs, R.D. *Site Index Curves for Forest Tree Species in the Eastern United States*; General Technical Report NC-128; US Department of Agriculture, Forest Service, North Central Forest Experiment Station: St. Paul, MN, USA, 1989.
49. Noordermeer, L.; Bollandasås, O.M.; Gobakken, T.; Næsset, E. Direct and indirect site index determination for Norway spruce and Scots pine using bitemporal airborne laser scanner data. *For. Ecol. Manag.* **2018**, *428*, 104–114. [[CrossRef](#)]
50. Næsset, E. Predicting forest stand characteristics with airborne scanning laser using a practical two-stage procedure and field data. *Remote Sens. Environ.* **2002**, *80*, 88–99. [[CrossRef](#)]
51. Riaño, D.; Meier, E.; Allgöwer, B.; Chuvieco, E.; Ustin, S.L. Modeling airborne laser scanning data for the spatial generation of critical forest parameters in fire behavior modeling. *Remote Sens. Environ.* **2003**, *86*, 177–186. [[CrossRef](#)]
52. Hopkinson, C.; Chasmer, L.; Lim, K.; Treitz, P.; Creed, I. Towards a universal lidar canopy height indicator. *Can. J. Remote Sens.* **2006**, *32*, 139–152. [[CrossRef](#)]
53. Fox, T.R.; Jokela, E.J.; Allen, H.L. The development of pine plantation silviculture in the southern United States. *J. For.* **2007**, *105*, 337–347.
54. Fox, T.R.; Kyle, K.H.; Andrews, L.J.; Aust, W.M.; Burger, J.A.; Hansen, G.H. Long-term effects of drainage, bedding, and fertilization on growth of loblolly pine (*Pinus taeda* L.) in the Coastal Plain of Virginia. *South. J. Appl. For.* **2005**, *29*, 205–214.

55. Albaugh, T.J.; Fox, T.R.; Allen, H.L.; Rubilar, R.A. Juvenile southern pine response to fertilization is influenced by soil drainage and texture. *Forests* **2015**, *6*, 2799–2819. [[CrossRef](#)]
56. NRCS. *National Soil Survey Handbook (Title 430-VI)*; U.S. Department of Agriculture: Washington, DC, USA, 2007.
57. Norby, R.J.; Zak, D.R. Ecological lessons from free-air CO<sub>2</sub> enrichment (FACE) experiments. *Annu. Rev. Ecol. Evol. Syst.* **2011**, *42*, 181. [[CrossRef](#)]
58. Murthy, R.; Dougherty, P.M.; Zarnoch, S.J.; Allen, H.L. Effects of carbon dioxide, fertilization, and irrigation on photosynthetic capacity of loblolly pine trees. *Tree Physiol.* **1996**, *16*, 537–546. [[CrossRef](#)] [[PubMed](#)]
59. Thomas, R.Q.; Canham, C.D.; Weathers, K.C.; Goodale, C.L. Increased tree carbon storage in response to nitrogen deposition in the US. *Nat. Geosci.* **2010**, *3*, 13. [[CrossRef](#)]
60. Subedi, S.; Fox, T.R.; Wynne, R.H. Determination of fertility rating (FR) in the 3-PG model for loblolly pine plantations in the southeastern United States based on site index. *Forests* **2015**, *6*, 3002–3027. [[CrossRef](#)]



© 2019 by the authors. Licensee MDPI, Basel, Switzerland. This article is an open access article distributed under the terms and conditions of the Creative Commons Attribution (CC BY) license (<http://creativecommons.org/licenses/by/4.0/>).